Preprint Title Chitosan-Glutathione nanoparticles modify oxidative stress induced by doxorubicin in breast cancer cells

Authors Laura D. López-Barrera, Roberto Díaz-Torres, Joselo R. Martínez-Rosas, Ana M. Salazar Martínez, Carlos Rosales and Patricia Ramirez-Noguera

Publication Date 06 Mär 2020

Article Type Full Research Paper

ORCID® iDs Laura D. López-Barrera - https://orcid.org/0000-0001-5445-3636; Roberto Díaz-Torres - https://orcid.org/0000-0002-1746-806X; Patricia Ramirez-Noguera - https://orcid.org/0000-0002-0900-9162

Chitosan-Glutathione nanoparticles modify oxidative stress induced by doxorubicin in breast cancer cells

López-Barrera, L. D. *[1], Díaz-Torres, R.‡[1], Martínez-Rosas J. R.‡[1], Salazar A.M. ‡[2], Rosales, C. ‡[3], Ramírez-Noguera, P. *[1]

Address: [1]Departamento de Ciencias Biológicas, Facultad de Estudios Superiores Cuautitlán, Universidad Nacional Autónoma de México (UNAM), México.

[2] Departamento de Medicina Genómica y Toxicología ambiental, Instituto de Investigaciones Biomédicas, Universidad Nacional Autónoma de México (UNAM), México.

[3] Departamento de Inmunología, Instituto de Investigaciones Biomédicas, Universidad Nacional Autónoma de México (UNAM), México.

Email: Patricia Ramirez-Noguera – ramireznoguera@unam.mx

* Corresponding author

‡ Equal contributors

Abstract

Doxorubicin is a widely used antineoplastic agent for the treatment of various types of cancer. However, it is also a highly toxic drug because it induces the generation of oxidative stress. Thus, the use of antioxidant molecules has been considered to reduce the toxicity of doxorubicin. In this report, we investigated whether the use of chitosan-glutathione (CH-GSH) nanoparticles could reduce cell damage induced by doxorubicin

on breast cancer cells. CH-GSH NPs were characterized in size, Zeta potential, concentration, and shape. When breast cancer cells were treated with CH-GSH nanoparticles, these were localized in the cellular cytoplasm. Combined exposure of doxorubicin and nanoparticle increased intracellular GSH levels while decreasing reactive oxygen species and malondialdehyde levels. The antioxidant enzyme activity was also decreased. Together our data suggest that the use of CH-GSH nanoparticles can reduce the oxidative stress induced by doxorubicin on breast cancer cells.

Keywords

Doxorubicin; oxidative stress; nanoparticles; glutathione; chitosan

Introduction

Breast cancer is one of the leading health problems worldwide. Its incidence is estimated at 11.6%, placing it among the first three types of cancer diagnosed in both men and women [1]. Approximately half of the people diagnosed with breast cancer usually presents recurrences even after treatment, and about one-third of these patients die from the disease [2]. About 80 % of breast carcinomas are positive for hormonal (progesterone and estrogen) receptors. These tumors are treated with drugs, such as tamoxifen, that block estrogen-induced cell growth. Other breast tumors (about 15 %) express the epidermal growth factor receptor (HER2). These tumors are treated with the monoclonal antibody trastuzumab, which is specific against HER2. The third group of breast tumors does not express hormonal receptors nor HER2 and thus are known as triple-negative. These tumors tend to be more aggressive, and their treatment is based on the general inhibition of cell replication on all dividing cells [2].

Doxorubicin is a potent broad-spectrum antineoplastic agent belonging to the anthracycline family, that is used for the treatment of various types of cancer, including breast cancer. Its mechanism of action is associated with inhibition of cell replication by binding to the enzyme topoisomerase II and thus causing DNA alterations and favoring the aging of cells [3]. Unfortunately, it also induces oxidative stress that can affect both dividing and non-dividing cells [4]. As a consequence, doxorubicin can trigger undesirable side effects due to general cell toxicity. Doxorubicin stimulates the formation of free radicals and reactive oxygen species (O_2^-, H_2O_2, and •OH) through Fenton chemistry reactions. Besides, this antineoplastic can activate the NADPH oxidase and modify calcium metabolism [4]. There is a growing interest in finding ways of reducing oxidative stress in tissues during doxorubicin treatment. A promising approach is the use of antioxidant molecules [5,6]. In particular, glutathione (GSH) is one of the primary endogenous antioxidants at the cellular level and is associated with various events such as proliferation, apoptosis, and redox state regulation. It is synthesized exclusively in the cell cytoplasm, once used and in its oxidized state, it cannot be incorporated into the cell so it must be synthesized to keep the levels in an optimal state [7]. Glutathione (GSH) is recognized as a critical antioxidant molecule for cell protection from toxins, both endogenous and environmental, including several anti-cancer cytotoxic drugs [8].

Transporting GSH and other agents to cells in order to reduce the toxic effects of anti-cancer drugs requires the use of innovative delivery systems [9]. The use of nanotechnology in cancer treatment represents a novel alternative to deliver agents to cells, thanks to the physicochemical properties that many different types of nanoparticles have [10]. Chitosan (CH), a natural polymer, has been used to create

nanoparticles that are ideal delivery systems because they are easy to produce, have a shallow immunogenic profile, diffuse quickly into cells, and are biodegradable and biocompatible [11]. Also, CH nanoparticles can easily interact with many other molecules due to their chemical structure [11]. Chitosan nanoparticles have already been reported to deliver molecules that can regulate events associated with inflammation [12] and can sensitize cancer cells to X-ray radiation [13].

In this report, we explored the use of CH-GSH nanoparticles to reduce the oxidative stress induced by doxorubicin on two breast cancer cell lines. Combined exposure of doxorubicin and CH-GSH nanoparticles increased intracellular GSH levels while decreasing reactive oxygen species and malondialdehyde levels. The antioxidant enzyme activity was also decreased. Our data suggest that the use of CH-GSH nanoparticles can reduce the oxidative stress induced by doxorubicin on breast cancer cells.

Results and Discussion

Chitosan (CH)-glutathione (GSH) nanoparticles were prepared according to the ionic gelation method described in the experimental section. Nanoparticles were characterized by measuring their size, polydispersion index (PDI), the Zeta potential, concentration, and the percentage of GSH encapsulation (Table 1). Both CH-GSH nanoparticles and CH-GSH nanoparticles labeled with rhodamine 123 had a size between 100-150 nm. The particle size is an important parameter since it is assumed that most nanoparticles can be transported into the cells by endocytosis [14]. The polydispersion index indicated that both preparations of nanoparticles were homogeneous suspensions. This argument was further supported by the Zeta

potential, which suggested that the nanoparticles remained in suspension without precipitation [15]. The percentage of GSH encapsulation was 99.23%, indicating that enough GSH was captured in the nanoparticles. Since GSH is very hydrophilic, it cannot enter cells unless it is trapped inside a nanocarrier. Also, the characterization of the nanoparticles by transmission electron microscopy showed that most particles were spherical (Figure 1).

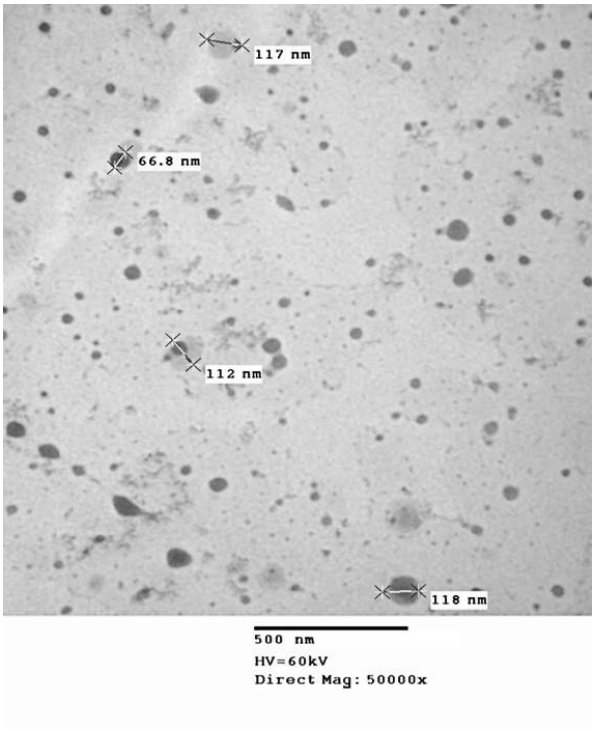

Figure 1: Image of Transmission electron microscopy of CH-GSH NPs

Table 1: Characterization results

Nanoparticles	Size (nm)	PDI	Z potential (mV)	Amount of NP (NPs/mL)	Encapsulation of GSH (%)
CH-GSH NPs	147.1	0.246	15.2	3.718×10^{10}	99.23

CH-GSH NPs R-123	129.8	0.264	23.2	$5.343x10^{10}$	99.23

Internalization of nanoparticles by cells

Cells were exposed to two different concentrations of CH-GSH nanoparticles labeled with rhodamine-123 for 2 hours and subsequently stained with DAPI to differentiate the nucleus. Two different breast cancer cell lines readily internalized the nanoparticles, which accumulated in the cytoplasm near to the periphery of the nucleus. As shown in Figure 2 (A and B), CH-GSH NPs are in the cytoplasm, in both cell lines. We used two different concentrations of nanoparticles; however, no significant differences were observed in the images obtained. It has been suggested that the interaction of chitosan with cells may occur through two mechanisms [16]. The first one consists of the interaction of positive charges of chitosan with the cellular membrane, and the second one consists of the bind of chitosan with some membrane receptor related to endocytosis. These mechanisms could be associated with the intracellular translocation of CH-GSH NPs. The vectorization can also be favored by the presence of the thiol group that can form disulfide bonds with glycoproteins in the cell membrane, improving its uptake [17].

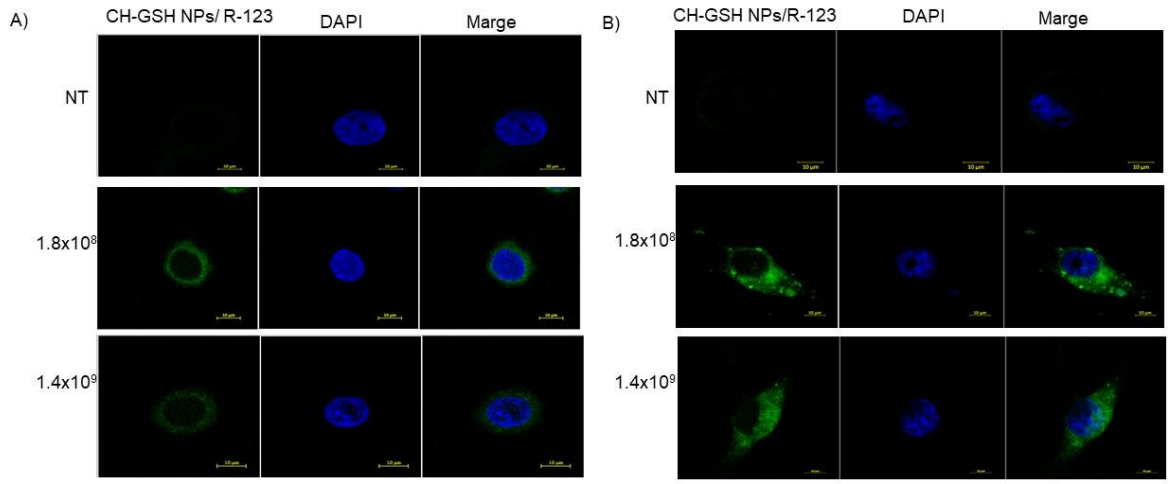

Figure 2: Confocal microscopy images of cells exposed to a concentration of $1.8x10^8$ NPs/mL (equal at 0.08 mM of GSH) and $1.4x10^9$ NPs/mL (equal at 0.64 mM of GSH) on time of 2 hrs, Untreated cells (NT). A) MCF-7 and B) MDA-MB-231 cells.

Intracellular and extracellular GSH concentrations

Once it was determined that the CH-GSH nanoparticles were internalized by cells, it was essential to evaluate the delivery of GSH into the cells. Total intracellular and extracellular GSH concentrations were determined in cells exposed to the nanoparticles. Extracellular GSH was barely detectable in all conditions for MCF-7 cells (Figure 3B) and MDA-MB-231 cells (Figure 3D). This finding indicates that the nanoparticles do not leak the GSH. Intracellular GSH concentration did not increase with a low dose of nanoparticles compared with the control. However, with a higher dose of nanoparticles, intracellular GSH increased somehow in MCF-7 cells (Figure 3A). For MDA-MB-231 cells, the nanoparticle treatment did not change the intracellular concentration of GSH (Figure 3C). These results suggest differences in the susceptibility of exposed cells by having available GSH content in the nanoparticles.

Probably even though the nanoparticles are inside the cells, GSH is not released quickly. The exposure of CH-GSH NPs at a concentration of $1.8x10^8$ does not modify GSH intracellular levels compared to untreated cells (NT), this occurs in both cell lines. However, exposure to the concentration of $1.4x10^9$ increases GSH levels significantly in MCF-7 cells.

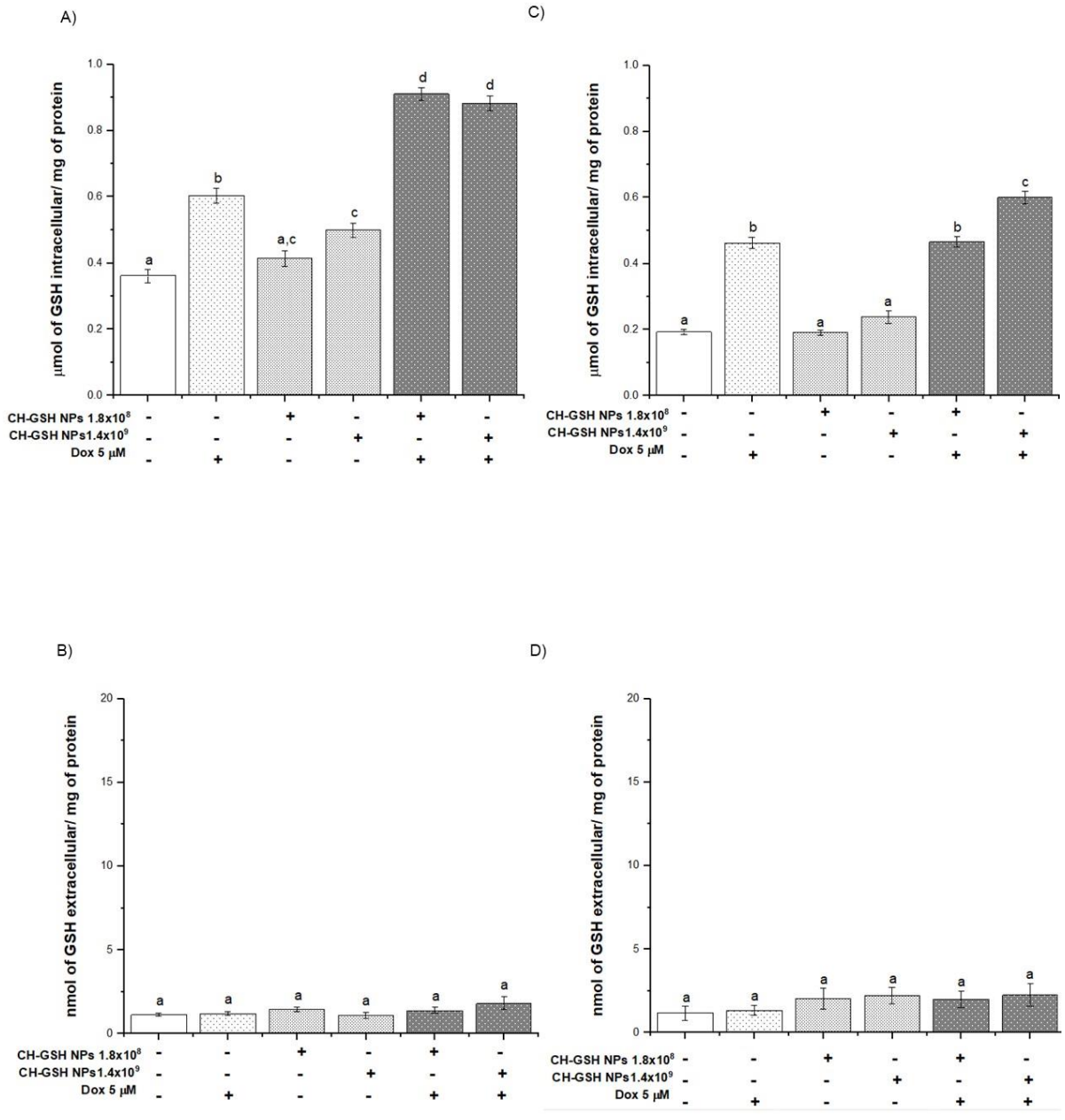

Figure 3: GSH intra and extracellular levels of cells exposed to doxorubicin for 12 hrs and then 2 hrs with CH-GSH NPs. (A, B) MCF-7 and (C, D) MDA 231 cells. Bars with equal letters indicate that there are no significant differences between the means (Tukey test, $p < 0.05$)

Exposing cells to doxorubicin increased significantly intracellular GSH concentration (Figure 3). Since doxorubicin can activate the NADPH oxidase and induce the formation of reactive oxygen species, the cell seems to respond by producing more antioxidant GSH [18, 19].

Combined exposure to doxorubicin and CH-GSH nanoparticles increased GSH concentration even more than exposure to doxorubicin alone. This increase was more evident in MCF7 cells than in MDA-MB-231 cells (Figure 3). This finding suggests that when cells have internalized CH-GSH nanoparticles and are treated with doxorubicin, the nanoparticles become an additional source of the antioxidant GSH. Doxorubicin modified intracellular GSH levels due to its mechanism of action associated with the generation of reactive oxygen species [19]. The increase in GSH levels could be due to the exposition to CH-GSH NPs, or the enhances of cytotoxic effects induced by combinatorial exposure of doxorubicin and GSH mentioned in other works [20].

We quantified the extracellular GSH levels in the culture medium used in cells exposed to doxorubicin and NPs. In Figure 3 (B, D) is shown that there are no significant differences between extracellular GSH levels in any of the culture media for the treatments and any cell lines used. The contrast between intracellular and extracellular GSH values suggests the inclusion of nanoparticles and correlates with confocal microscopy images and suggests the bioavailability of thiol contained in nanoparticles.

We observed differential cellular sensitivity to the exposure to the biological effects induced by the nanoparticles and in combination with doxorubicin.

Malondialdehyde concentration

Malondialdehyde (MDA) is a final product of lipid oxidation. Thus, it is an indicator of cellular damage due to oxidative stress [21]. Treating MCF7 cells with doxorubicin resulted in a marked increase in malondialdehyde concentration (Figure 4A). A similar result was observed in MDA-MB-231 cells (Figure 4B). Exposure of cells to the CH-GSH nanoparticles did not change the basal concentration of malondialdehyde (Figure 4), indicating that the nanoparticles alone did not induce oxidative stress on the cells. Combined exposure to doxorubicin and subsequently to CH-GSH nanoparticles resulted in a substantial reduction of malondialdehyde concentration (Figure 4). This result indicates that CH-GSH nanoparticles offer a protective antioxidant effect.

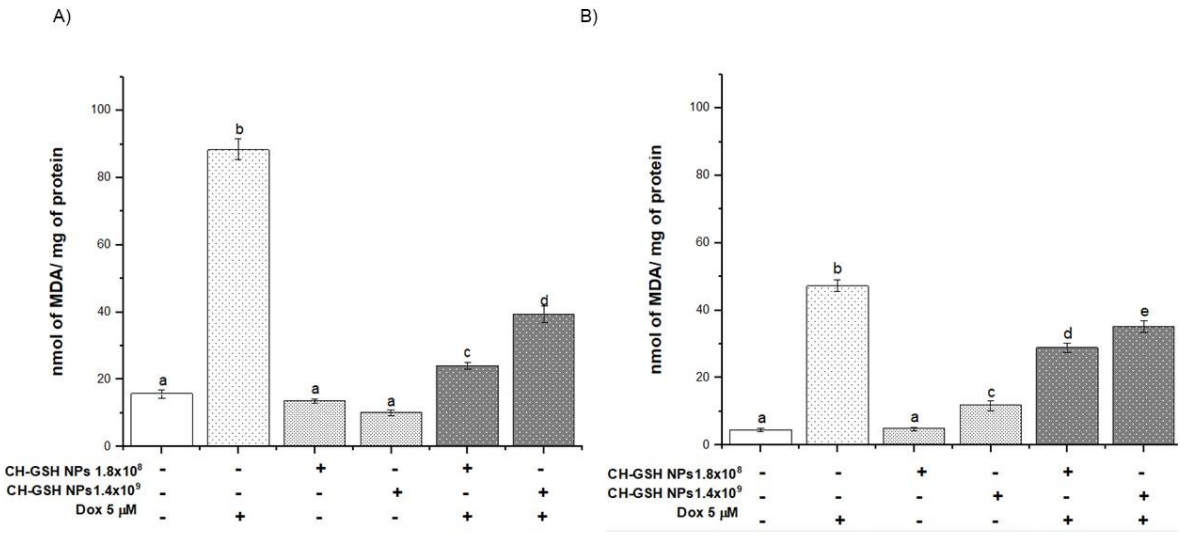

Figure 4: Malondialdehyde levels of cells exposed to doxorubicin for 12 hrs and then 2 hrs with CH-GSH NPs. A) MCF-7 and B) MDA 231 cells. Bars with equal letters

indicate that there are no significant differences between the means (Tukey test, $p < 0.05$)

In Figure 4 (A, B), cells exposed to CH-GSH NPs maintained levels of malondialdehyde significantly like untreated cells, while exposure to doxorubicin increased MDA levels in both cell lines significantly. The GSH into NPs could interact directly with reactive oxygen species and free radical or be used by antioxidant enzymes to reduce oxidative stress produced by doxorubicin exposition [7]. We observed the effect in both cell lines, and both concentrations of NPs tested.

On the other hand, cell lines such as MDA-MB-231 used to study the basal subtype have shown to be metabolically more active, and have a better adaptive response to drug treatments [22], so MCF-7 cells may be more sensitive to exposure to CH-GSH NPs, as observed at intracellular GSH levels and now at MDA levels.

Measurement of reactive oxygen species

If the nanoparticles under study were able to modify the amount of intracellular GSH and the number of species reactive to barbituric acid decreased significantly in the combined exposures compared to doxorubicin alone. We decided to estimate the amount of ROS using 2, 7 dichlorofluorescein diacetate (DCFDA).

In Figure 5 (A, B) is shown normalized results considering untreated cells as baseline ROS levels. Cells exposed to CH-GSH nanoparticles did not change the amount of basal showed ROS levels (Figure 5). As anticipated, cells exposed to doxorubicin had

a higher amount of ROS (Figure 5). In contrast, the combined exposure to doxorubicin and CH-GSH nanoparticles resulted in a marked reduction of ROS levels (Figure 5), implying that at the cellular level, modulator effects are modifying the amount of ROS due to the exposure of CH-GSH nanoparticles indeed induce a protective antioxidant effect in cells exposed to doxorubicin.

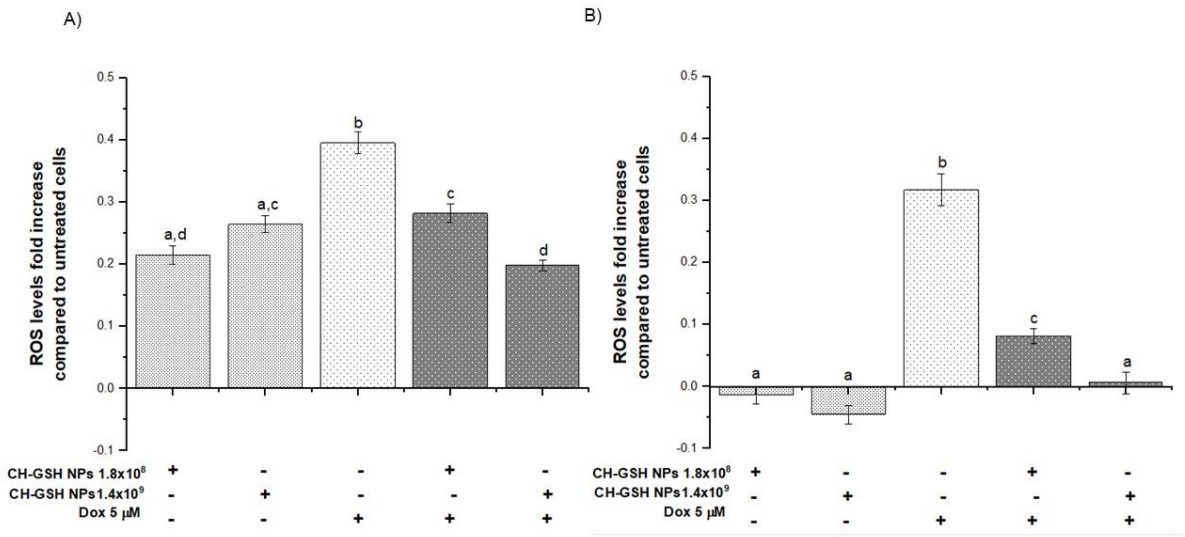

Figure 5: ROS levels fold increase compared to untreated cells. The cells were exposed to doxorubicin for 12 hrs and then 2 hrs with CH-GSH NPs. A) MCF-7 and B) MDA 231 cells. Bars with equal letters indicate that there are no significant differences between the means (Tukey test, $p < 0.05$)

Doxorubicin induces oxidative stress through the formation of radicals and ROS due to the metabolic transformation of doxorubicin to doxorubicinol, which generates an increase in the release of iron, producing free radicals through non-enzymatic mechanisms associated with this metal [18].

In addition to the GSH, NPs are made of chitosan, which in various works has been reported to have antioxidant properties, due to its ability to provide ligand in the amino and hydroxyl groups in position C-3 and C-2 and effective chelation of heavy metals like Fe^{2+} [23]. It has also reported that these groups may be responsible for the entrapment of some free radicals [24].

The results suggested a higher sensitivity to the exposure of NPs of MCF-7 cells; maybe due to cell line, some reports suggested an increase in metabolism associated with redox pathways in triple-negative cells such as MDA-MB-231 compared to those that are positive to estrogen receptors such as MCF-7 cells [22].

Catalase Activity

Catalase is the enzyme responsible for the degradation of H_2O_2 to H_2O. Thus, it has a protective antioxidant effect in the cell. The basal activity of catalase in MCF-7 cells did not change after exposing the cells to CH-GSH nanoparticles (Figure 6A). In contrast, catalase activity in MDA-MB-231 cells was increased by exposing the cells to the nanoparticles (Figure 6B). This variation in response reflects important metabolic differences in both cell lines. Despite this, both cell lines presented a marked increase in catalase activity after treatment with doxorubicin (Figure 6), which was inhibited by the presence of the nanoparticles (Figure 6).

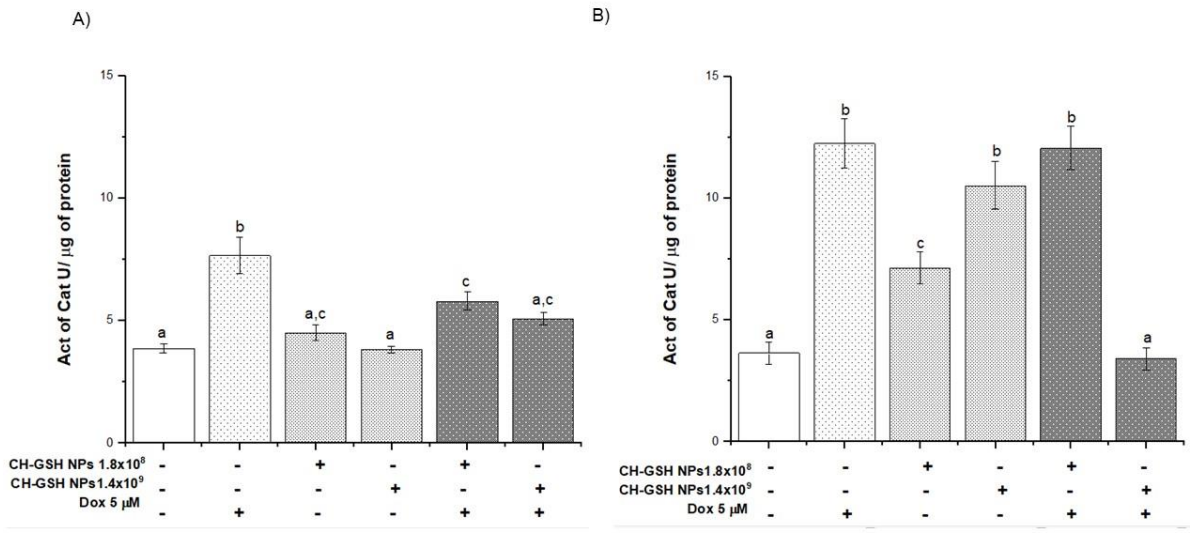

Figure 6: Activity of Catalase. The cells were exposed to doxorubicin for 12 hrs and then 2 hrs with CH-GSH NPs. (A) MCF-7 and (B) MDA 231 cells. Bars with equal letters indicate that there are no significant differences between the means (Tukey test, $p < 0.05$)

We quantified the specific activity of catalase according to the technique of Iwase [25]. In Figure 6, exposure of CH-GSH NPs only modified the activity of MDA-MB-231 cells, while in MCF-7 cells, there is no difference in respect to untreated cells. However, when cells exposed to doxorubicin and CH-GSH NPs, the activity is diminished compared to doxorubicin-induced.

As previously observed, the GSH from NPs modified ROS levels, so the activity of catalase could decrease for this reason. It has been reported in isolates of catalase enzyme that the exposition with chitosan facilitates the binding covalently to the enzyme; amino groups that are present in the chitosan immobilize or trap this enzyme and modify its activity [26, 27].

Glutathione Peroxidase Activity

The method described by R. S. Esworthy was used to determine the activity of GPx [28].

In Figure 7, we can observe that the enzyme activity only modified MDA-MB-231 cells in a concentration of $1.8x10^8$. When cells exposed to doxorubicin in combination with CH-GSH NPs, the activity increase in levels like doxorubicin-induced in MCF-7 cells, and the activity decreased in MDA-MB-231 cells.

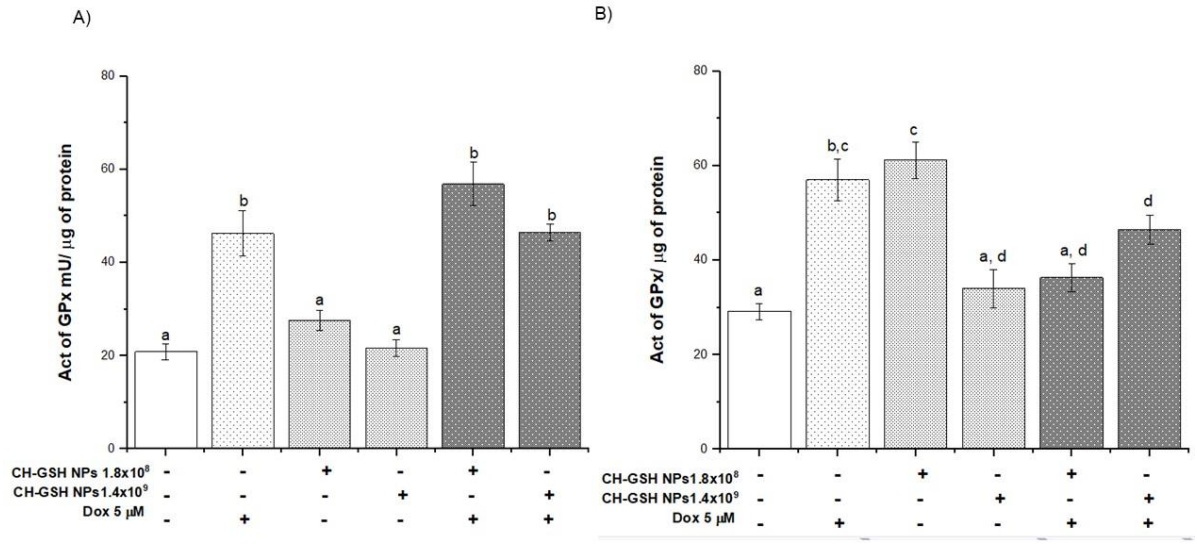

Figure 7: Glutathione Peroxidase activity. The cells were exposed to doxorubicin for 12 hrs and then 2 hrs with CH-GSH NPs. (A) MCF-7 and (B) MDA 231 cells. Bars with equal letters indicate that there are no significant differences between the means (Tukey test, $p < 0.05$)

The enzyme Glutathione peroxidase (GPx) is part of the intrinsic antioxidant mechanisms of a cell, by reducing peroxides with the aid of GSH as a reducing agent at the cellular level. The basal activity of glutathione peroxidase in MCF-7 cells did not change after exposing the cells to CH-GSH nanoparticles (Figure 7A). In contrast, glutathione peroxidase activity in MDA-MB-231 cells was increased after exposing the cells to a concentration of $1.8x10^8$ nanoparticles (Figure 7B). Again, this variation in response seems to reflect important metabolic differences in both cell lines. Both cell lines presented a marked increase in glutathione peroxidase activity after treatment with doxorubicin (Figure 7), which was not inhibited by the presence of the nanoparticles in MCF-7 cells (Figure 7A). In contrast, the nanoparticles induced a significant decrease in glutathione peroxidase activity in MDA-MB-231 cells after treatment with doxorubicin (Figure 7B).

This selenium-dependent enzyme has the function of carrying out the detoxification of hydrogen peroxide and endogenously formed hydroperoxides. The GPx reduces peroxides by using GSH as a reducing agent, which is oxidized and converted into disulfide glutathione (GSSG) and is later regenerated by the enzyme Glutathione reductase (GRx) [29]. The decrease in activity may be due to the reduction in the amount of ROS, and it is more evident in MDA-MB-231 cells that, as mentioned above has a better response to modifications of the redox state.

Glutathione Reductase Activity

Glutathione (GSH) functions as a reducing agent during the elimination of peroxides by being oxidized and converted into disulfide glutathione (GSSG). Later, the enzyme glutathione reductase uses GSSG as a substrate to regenerate GSH [28]. Glutathione reductase is induced under oxidative stress [30]. Thus, its activity is also indicative of

the antioxidant state of a cell. The basal activity of glutathione reductase in MCF-7 cells and MDA-MB-231 cells did not change after exposing the cells to CH-GSH nanoparticles (Figure 8). Both cell lines presented a marked increase in glutathione peroxidase activity after treatment with doxorubicin, which was completely blocked in the presence of the nanoparticles. The result suggested, the nanoparticles induced a decrease in the amount of ROS in the cell, and as a consequence, the cell did not require the activation of glutathione peroxidase.

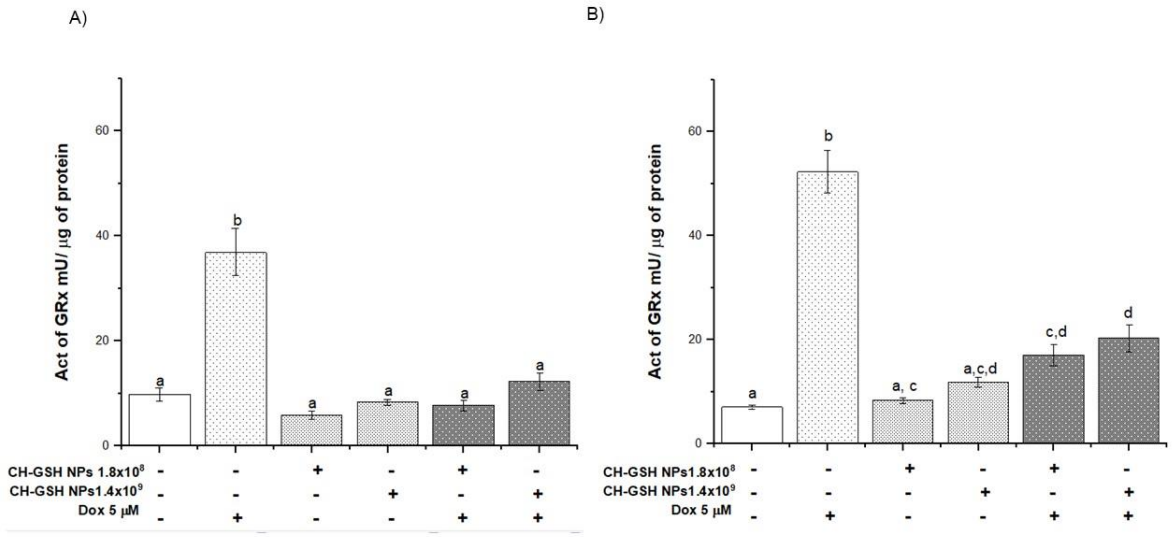

Figure 8: Glutathione Reductase activity. The cells were exposed to doxorubicin for 12 hrs and then 2 hrs with CH-GSH NPs. (A) MCF-7 and (B) MDA 231 cells. Bars with equal letters indicate that there are no significant differences between the means (Tukey test, $p < 0.05$)

MCF-7 cells showed increased sensitivity to the exposure of nanoparticles in comparison with MDA 231 cells in the various tests performed. This finding may be due to its metabolism, and it has reported that doxorubicin modifies the metabolism of

both cell lines by affecting more the metabolic profile of MDA-MB-231 cells than in MCF7 cells, showing changes in ketonic bodies, glycolysis and in the energetic and lipid metabolism [31, 32]. Also, MDA-M- 231 cells have a higher consumption of glucose and upregulated of redox pathways in comparison with MCF-7 [33].

On the other hand, the observed effect may be due, as mentioned by some authors, that combined exposure of nanoparticles with various agents enhance the sensibilization of cells. Zelbielca et al. showed that combined exposure of nanoparticles of doxorubicin/GSH has higher cytotoxic effects than free doxorubicin in feline fibrosarcoma cell lines [20]. In a study in MCF-7 cells with metallic nanoparticles and radiation, there was a higher effect on the combination exposure, acting nanoparticles as nano-sensitizers [34]. Suganya et al. suggest that gold nanoparticles act as sensitizing agents in MDA-MB-231 and MCF-7 cells, modifying cell-cycle effects, viability, and DNA damage [35]. Alvandifar et al. used a combined exposition of PLGA and verapamil nanoparticles to improve the effectiveness of this chemotherapeutic and decrease the dose to have higher effects. These results suggest that the combined exposure of nanoparticles and this chemotherapeutic increase the expression of BAX and reduce levels of BCL2, suggesting that the nanoparticles' advantage is that they decrease the resistance of MDA 231 cells to this type of drugs [36].

Conclusion

The results obtained suggest that CH-GSH NPs modulate the cellular redox state, reducing the oxidative stress generated by the exposure of doxorubicin. There was

also a higher sensitivity of MCF-7 cells to CH-GSH NPs compared to MDA-MB-231 cells; this may be due to the genotypic characteristics of each cell. However, more studies are required to understand the effect of exposure of CH-GSH-NPS on other cellular events associated with the mechanisms of action of doxorubicin like apoptosis and cell proliferation. In the future, CH-GSH NPs could serve as adjuvants to modify the toxic effects generated by this antineoplastic in the treatment of cancer.

Experimental

Preparation and characterization of nanoparticles

Chitosan-glutathione (CH-GSH) nanoparticles were prepared by the ionic gelation technique, as previously described [37]. CH-GSH nanoparticles were also coupled to rhodamine-123 at a concentration of 0.5 mg/ml in methanol, for confocal microscopy analysis. Then, nanoparticles were characterized, in concentration, size, and zeta potential using the equipment Nanosight and Zetasizer from Malvern instrument. Quantification of encapsulated GSH was determined indirectly by the DTNB technique at a wavelength of 425 nm [38]. Finally, were observed the shape of CH-GSH nanoparticles through transmission electron microscopy.

Cell lines and culturing

The breast cancer cell lines MCF-7 (ATCC HTB-22) and MDA-MB-231 (ATCC HTB-26) were used. MCF-7 cells are positive for functional estrogen receptors, and MDA-MB-231 cells are negative for estrogen receptor, progesterone receptor, and E-cadherin. Cells were cultured in DMEM medium, supplemented with 12% fetal bovine serum (FSB), at 37°C in a 5% CO_2 incubator. Cells were cultured in either 24-well or

6-well tissue culture plates until they were confluent before performing the various assays described next

Confocal microscopy analysis

Nanoparticles coupled to rhodamine-123 were added to MCF-7 and MDA-MB-231 cells, two concentrations of nanoparticles were used $1.8x10^8$ nanoparticles/ml (equivalent to 0.08 mM GSH) and $1.4x10^9$ nanoparticles/ml (equivalent to 0.64 mM GSH) for 2 hours. Then, cells were washed with PBS, fixed with 3% paraformaldehyde, and stained with DAPI (0.1µg/ml). Finally, cells were observed with a confocal microscopy LSM Zeiss 800.

Intracellular and extracellular GSH concentrations

Confluent cells cultured in 6-well plates were scraped and placed in 100µl lysis buffer (0.1% Triton, 5 mM EDTA, 1 mM PMSF). Cells were centrifuged at 13 000 rpm, 10 min 4°C and cell lysate transferred to a clean tube. The amount of total protein in cell lysates was determined according to Bradford's method [39].

The concentration extracellular of GSH was measured indirectly using the culture medium of the cells that were treated with nanoparticles. The concentration of intracellular and extracellular GSH was determined with the 2,2-dithiobisnitrobenzoic acid (DTNB) assay [38]. This assay is based on the reaction of GSH with DTNB, forming a yellow adduct product (GS-TNB), that can be read spectrophotometrically at a wavelength of 425 nm.

Malondialdehyde concentration

Malondialdehyde concentration was determined with the thiobarbituric acid reactive species (TBARS) assay [21], with some modifications. Thiobarbituric acid was added to the samples at a concentration of 0.67%, and then samples were incubated at 90°C for 30 min. This assay is based on the reaction of malondialdehyde with thiobarbituric acid to form a pink adduct product. The product can be read spectrophotometrically at a wavelength of 540 nm.

Measurement of reactive oxygen species

Detection of reactive oxygen species was performed with the 2, 7 dichlorofluorescein diacetate (DCFDA) assay [40], with some modifications. DCFDA was added to the cells at a concentration of 5 μM and then cells were incubated for 15 min at 37 ° C. In the presence of reactive oxygen species and other peroxides, DCFDA is oxidized to 2,7-dichlorofluorescein (DCF), a fluorescent product that can be detected with a fluorometer at excitation light ʎex = 488 nm and emission light ʎem = 525 nm.

Catalase activity

Catalase (Cat) activity was estimated as previously reported [25]. Briefly, samples with catalase in 200 μL of a reaction medium containing triton x-100 (1%) and PBS were incubated at 37°C for 15 minutes, and then 100 μL of a 30% H_2O_2 solution were added. The enzyme-generated oxygen bubbles trapped by triton X-100 were visualized as foam, whose height was estimated. A calibration generated with known catalase activity units is used to interpolate the foam height and estimate the catalase activity in each sample.

Glutathione Peroxidase activity

The activity of the enzyme glutathione peroxidase (GPx) was estimated as previously reported [28]. The technique is based on the measurement of the decrease in absorption of NADPH by a coupled reaction with the GPx. The GPx uses GSH to convert H_2O_2 to H_2O. As a result, GSSG produced is regenerated by GRx with the conversion of NADPH to $NADP^+$. A wavelength of 340 nm is used for the reading.

Glutathione Reductase Activity

The activity of the enzyme glutathione reductase (GRx) was estimated as previously reported [41]. Confluent cells cultured in 6-well plates were scraped and placed in 100 µl lysis buffer (0.1% Triton, 5 mM EDTA, 1mM PMSF). Cells were centrifuged at 13000 rpm, 10 min, 4°C, and cell lysate transferred to a clean tube. The activity of glutathione reductase results in the reduction of the oxidized form of glutathione, disulfide glutathione (GSSG), to reduced glutathione. Since this reaction is coupled to the oxidation of NADPH, and NADPH absorbs light at 340 nm, a decrease in absorbance reflects its oxidation.

Statistical analysis

Results were analyzed using a one-way analysis of variance (ANOVA), followed by multiple comparisons of means according to the Tukey statistical test, considering a significant difference at $p<0.05$.

Funding

This work was funded by Grants PAPIME PE102118, and PAPIIT IN219715 from Dirección General de Asuntos del Personal Académico, Universidad Nacional Autónoma de México.

References

1. Bray, F.; Ferlay, J.; Soerjomataram, I.; Siegel, R. L.; Torre, L. A.; Jemal, A. *CA: A Cancer Journal for Clinicians* **2018**, *68* (6), 394–424. https://doi.org/10.3322/caac.21492.
2. Pardee JD; *Understanding Breast Cancer. Cell biology and therapy—A visual approach*. Morgan & Claypool Life Sciences. San Rafael, California (USA), 2008.
3. Renu, K.; V.G., A.; P.B., T. P.; *European Journal of Pharmacology* **2018**, *818*, 241–253. https://doi.org/10.1016/j.ejphar.2017.10.043.
4. Chegaev, K.; Riganti, C.; Rolando, B.; Lazzarato, L.; Gazzano, E.; Guglielmo, S.; Ghigo, D.; Fruttero, R.; Gasco, A. *Bioorganic & Medicinal Chemistry Letters* **2013**, *23* (19), 5307–5310. https://doi.org/10.1016/j.bmcl.2013.07.070.
5. Zabielska-Koczywąs, K.; Dolka, I.; Król, M.; Żbikowski, A.; Lewandowski, W.; Mieczkowski, J.; Wójcik, M.; Lechowski, R.. *Molecules* **2017**, *22* (2), 253. https://doi.org/10.3390/molecules22020253.
6. Songbo, M.; Lang, H.; Xinyong, C.; Bin, X.; Ping, Z.; Liang, S. *Toxicology Letters* **2019**, *307*, 41–48. https://doi.org/10.1016/j.toxlet.2019.02.013.
7. Kalinina, E. V.; Chernov, N. N.; Novichkova, M. D. *Biochemistry Moscow* **2014**, *79* (13), 1562–1583. https://doi.org/10.1134/S0006297914130082.
8. Wu JH, Batist G. *Glutathione and glutathione analogues; therapeutic potentials*.

Biochim. Biophys. Acta. **2013,** 1830: 3350-3353.

9. Raj, S.; Khurana, S.; Choudhari, R.; Kesari, K. K.; Kamal, M. A.; Garg, N.; Ruokolainen, J.; Das, B. C.; Kumar, D. *Seminars in Cancer Biology* **2019**, S1044579X19302160. https://doi.org/10.1016/j.semcancer.2019.11.002.
10. Bose A & Wui Wong T. *Nanotechnology-Enabled Drug Delivery for Cancer Therapy*. Nanotechnology Applications for Tissue Engineering. Elsevier Inc. **2015,** 173-193.
11. Rahmani, S.; Hakimi, S.; Esmaeily, A.; Samadi, F. Y.; Mortazavian, E.; Nazari, M.; Mohammadi, Z.; Tehrani, N. R.; Tehrani, M. R. *International Journal of Pharmaceutics* **2019**, *560*, 306–314. https://doi.org/10.1016/j.ijpharm.2019.02.016.
12. Ma, L.; Shen, C.; Gao, L.; Li, D.; Shang, Y.; Yin, K.; Zhao, D.; Cheng, W.; Quan, D. *Colloids and Surfaces B: Biointerfaces* **2016**, *142*, 297–306. https://doi.org/10.1016/j.colsurfb.2016.02.031.
13. Piña Olmos, S.; Díaz Torres, R.; Elbakrawy, E.; Hughes, L.; Mckenna, J.; Hill, M. A.; Kadhim, M.; Ramírez Noguera, P.; Bolanos-Garcia, V. M. *Biomolecules* **2019**, *9* (5), 186. https://doi.org/10.3390/biom9050186.
14. Monopoli MP, Pitek AS, Lynch L, Dawson DA. *Formation and Characterization of the Nanoparticle–Protein Corona, in: Nanomater. Interfaces* . Biol. Methods Protoc. **2013**, 1025: 137–155.
15. Hans, M. L.; Lowman, A. M.. *Current Opinion in Solid State and Materials Science* **2002**, 9.
16. Moran, H. B. T.; Turley, J. L.; Andersson, M.; Lavelle, E. C. *Biomaterials* **2018**, *184*, 1–9. https://doi.org/10.1016/j.biomaterials.2018.08.054.
17. Choi, C.; Nam, J.-P.; Nah, J.-W. *Journal of Industrial and Engineering Chemistry* **2016**, *33*, 1–10. https://doi.org/10.1016/j.jiec.2015.10.028.

18. Chegaev, K.; Riganti, C.; Rolando, B.; Lazzarato, L.; Gazzano, E.; Guglielmo, S.; Ghigo, D.; Fruttero, R.; Gasco,. *Bioorganic & Medicinal Chemistry Letters* **2013**, *23* (19), 5307–5310. https://doi.org/10.1016/j.bmcl.2013.07.070.
19. Tacar, O.; Sriamornsak, P.; Dass, C. R.. *J Pharm Pharmacol* **2013**, *65* (2), 157–170. https://doi.org/10.1111/j.2042-7158.2012.01567.x.
20. Zabielska-Koczywąs, K.; Dolka, I.; Król, M.; Żbikowski, A.; Lewandowski, W.; Mieczkowski, J.; Wójcik, M.; Lechowski, R.. *Molecules* **2017**, *22* (2), 253. https://doi.org/10.3390/molecules22020253.
21. Ohkawa, H.; Ohishi, N.; Yagi, K. *Analytical Biochemistry* **1979**, *95* (2), 351–358. https://doi.org/10.1016/0003-2697(79)90738-3.
22. de Ruijter, T. C.; Veeck, J.; de Hoon, J. P. J.; van Engeland, M.; Tjan-Heijnen, V. *J Cancer Res Clin Oncol* **2011**, *137* (2), 183–192. https://doi.org/10.1007/s00432-010-0957-x.
23. Chang, S.-H.; Wu, C.-H.; Tsai, G.-J. *Carbohydrate Polymers* **2018**, *181*, 1026–1032. https://doi.org/10.1016/j.carbpol.2017.11.047.
24. Zhang, Y.; Ahmad, K. A.; Khan, F. U.; Yan, S.; Ihsan, A. U.; Ding, Q. *Chemico-Biological Interactions* **2019**, *305*, 54–65. https://doi.org/10.1016/j.cbi.2019.03.027.
25. Iwase, T.; Tajima, A.; Sugimoto, S.; Okuda, K.; Hironaka, I.; Kamata, Y.; Takada, K.; Mizunoe, Y. *Sci Rep* **2013**, *3* (1), 3081. https://doi.org/10.1038/srep03081.
26. Inanan, T. *Reactive and Functional Polymers* **2019**, *135*, 94–102. https://doi.org/10.1016/j.reactfunctpolym.2018.12.013.
27. Grigoras, A. G. *Biochemical Engineering Journal* **2017**, *117*, 1–20. https://doi.org/10.1016/j.bej.2016.10.021.

28. Esworthy RS, Chu FF, Doroshow JH *Analysis of Glutathione-Related Enzymes*. Curr. Protoc. Toxicol. 1999 00: 7.1.1-7.1.32.
29. Benhar, M. *Free Radical Biology and Medicine* **2018**, *127*, 160–164. https://doi.org/10.1016/j.freeradbiomed.2018.01.028.
30. Couto, N.; Wood, J.; Barber, J. *Free Radical Biology and Medicine* **2016**, *95*, 27–42. https://doi.org/10.1016/j.freeradbiomed.2016.02.028.
31. Maria, R. M.; Altei, W. F.; Selistre-de-Araujo, H. S.; Colnago, L. A. *Biochemistry* **2017**, *56* (16), 2219–2224. https://doi.org/10.1021/acs.biochem.7b00015.
32. Maria, R. M.; Altei, W. F.; Selistre-de-Araujo, H. S.; Colnago, L. A. *Journal of Pharmaceutical and Biomedical Analysis* **2017**, *146*, 324–328. https://doi.org/10.1016/j.jpba.2017.08.038.
33. Willmann, L.; Schlimpert, M.; Halbach, S.; Erbes, T.; Stickeler, E.; Kammerer, B.. *Journal of Chromatography B* **2015**, *1000*, 95–104. https://doi.org/10.1016/j.jchromb.2015.07.021.
34. Taher, F. A.; Ibrahim, S. A.; El-Aziz, A. A.; Abou El-Nour, M. F.; El-Sheikh, M. A.; El-Husseiny, N.; Mohamed, M. M. *International Journal of Biological Macromolecules* **2019**, *126*, 478–487. https://doi.org/10.1016/j.ijbiomac.2018.12.151.
35. K.S., U. S.; K., G.; V., G. K.; D., P.; C., A.; T., S. D.; V., K.; Changmai, N. *Applied Surface Science* **2016**, *371*, 415–424. https://doi.org/10.1016/j.apsusc.2016.03.004.
36. Alvandifar, F.; Ghaffari, B.; Goodarzi, N.; Ravari, N. S.; Karami, F.; Amini, M.; Souri, E.; Khoshayand, M. R.; Esfandyari-Manesh, M.; Jafari, R. M.; et al. *Journal of Drug Delivery Science and Technology* **2018**, *47*, 291–298. https://doi.org/10.1016/j.jddst.2018.07.019.

37. López-Barrera LD, Díaz-Torres R, Ramírez-Noguera P, López Macay A, López-Reyes AG, Olmos S. *Pharmazie*. **2019** 74: 406–411
38. Hu ML.*Measurement of Protein Thiol Groups and Glutathione in Plasma*. Methods in Enzymology.**1994**, 233: 380-385.
39. Bradford M.M. *Anal. Biochem*. **1976**, 72: 248–254.
40. Wang H & Joseph JA. *Free Radic. Biol. Med*. **1999**, 27: 612–616.
41. Mannervik B. *Curr. Protocols Toxicol*. **1999**. 7.2.1-7.2.4.